Journal of Medicinal Chemistry

Perspective

Cite This: J. Med. Chem. XXXX, XXX, XXX−XXX

pubs.acs.org/jmc

TASK Channels Pharmacology: New Challenges in Drug Design

Mauricio Bedoya,[†] Susanne Rinné,[‡] Aytug K. Kiper,[‡] Niels Decher,[‡] Wendy González,[†,§] and David Ramírez*[,∥]

[†]Centro de Bioinformática y Simulación Molecular (CBSM), Universidad de Talca, 1 Poniente No. 1141, 3460000 Talca, Chile

[‡]Institute for Physiology and Pathophysiology, Vegetative Physiology and Marburg Center for Mind, Brain and Behavior, MCMBB, Philipps-University of Marburg, Deutschhausstraße 2, Marburg 35037, Germany

[§]Millennium Nucleus of Ion Channels-Associated Diseases (MiNICAD), Universidad de Talca, 1 Poniente No. 1141, 3460000 Talca, Chile

[∥]Instituto de Ciencias Biomédicas, Facultad de Ciencias de la Salud, Universidad Autónoma de Chile, El Llano Subercaseaux 2801, Piso 6, 8900000 Santiago, Chile

ABSTRACT: Rational drug design targeting ion channels is an exciting and always evolving research field. New medicinal chemistry strategies are being implemented to explore the wild chemical space and unravel the molecular basis of the ion channels modulators binding mechanisms. TASK channels belong to the two-pore domain potassium channel family and are modulated by extracellular acidosis. They are extensively distributed along the cardiovascular and central nervous systems, and their expression is up- and downregulated in different cancer types, which makes them an attractive therapeutic target. However, TASK channels remain unexplored, and drugs designed to target these channels are poorly selective. Here, we review TASK channels properties and their known blockers and activators, considering the new challenges in ion channels drug design and focusing on the implementation of computational methodologies in the drug discovery process.

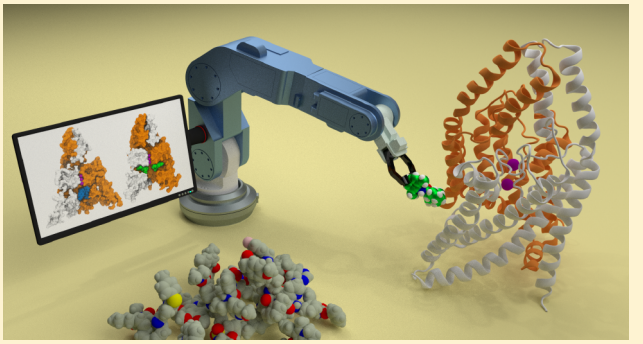

INTRODUCTION

Numerous cellular functions such as excitability, development, communication, homeostasis, and others are modulated by membrane proteins which create a gated, water-filled pore to regulate the membrane potential by controlling the ion flow between both the intracellular and extracellular environments.[1,2] These remarkable proteins are named ion channels. Potassium (K^+) channels form the largest family of ion channels as more than 80 genes in the human genome encode pore-forming subunits. They are classified into three main families according to their membrane topology:[3] (i) voltage-gated K^+ channels (K_v) and Ca^{2+}-dependent K^+ channels (K_{Ca}) with one pore domain and six transmembrane domains (1P/6TM) per subunit; (ii) inwardly rectifying K^+ channels (K_{ir}) with 1P/2TM per subunit; (iii) two-pore domain K^+ channels (K_{2P}) with 2P/4TM per subunit.[4] K_{2P} channels that include 15 mammalian members are divided into 6 subfamilies: TWIK (tandem of P domains in a weak inwardly rectifying K^+ channel), THIK (tandem-pore-domain halothane-inhibited K^+ channel), TREK (TWIK-related K^+ channel), TASK (TWIK-related acid-sensitive K^+ channel), TALK (TWIK-related alkaline-pH-activated K^+ channel), and TRESK (TWIK-related spinal-cord K^+ channel).[5,6] In this review, we focus on TASK channels. This subgroup of the *KCNK* gene family includes TASK-1 (also known as *KCNK3* and K_{2P}3.1), TASK-3 (*KCNK9* and K_{2P}9.1), and TASK-5 (*KCNK15* and K_{2P}15.1).[6,7] As homodimers or heterodimers, TASK-1 and TASK-3 generate archetypal K^+-selective leak currents, and TASK-5 subunits seem to be nonfunctional when expressed alone or together with other TASK subunits.[8] TASK channels play a principal role in extracellular pH sensitivity, oxygen sensitivity, apoptosis, mediation of general anesthesia, and tumorigenicity.[9,10] However, other K_{2P} channels such as TWIK-1, TALK, and TRESK have also been found to be sensitive to extracellular pH; hence, the use of pH sensitivity as a criterion of TASK identification has been redesigned.[6]

Ion channels are molecular targets of many drugs, and worldwide drug sales targeting ion channels exceed USD 12 billion.[11] However, due to the increased drug market, the significant demand for novel, most potent, and selective drugs, as well as the discovery and identification of approximately 400 ion channel pore-forming genes and accessory subunits, the rational drug design targeting ion channels rose over the past years. Thus, the new released K_{2P} crystal structures[12−16] as well as the development of new K_{2P} channel modulators[1,3,17−20] are the basis for new efforts regarding K_{2P} channels as novel therapeutic targets. This review presents an overview of TASK

Received: February 5, 2019
Published: July 1, 2019

DOI: 10.1021/acs.jmedchem.9b00248
J. Med. Chem. XXXX, XXX, XXX−XXX

channels, their function, physiological role, and structure; we also explore the primary TASK modulators reported and the challenges and future directions of the drug design targeting these channels.

TOPOLOGY AND STRUCTURE

The TASK subfamily of K_{2P} channels includes TASK-1, TASK-3, and TASK-5 with 394 amino acids (aa),[21] 374 aa,[22,23] and 330 aa,[24] respectively. In humans, TASK-1 shares 58.9% of aa sequence identity with TASK-3 and 51.4% with TASK-5; conversely, TASK-3 shares 55.1% of identity with TASK-5 (Figure 1). This close relationship is very similar in the TREK

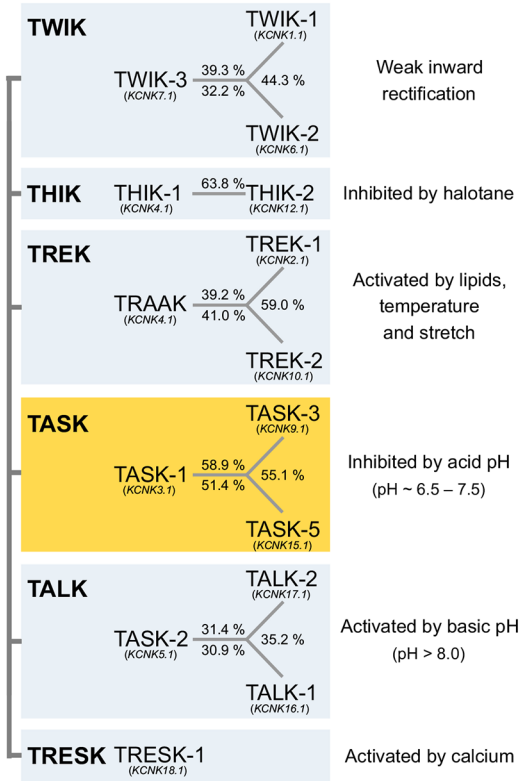

Figure 1. K_{2P} subfamilies in *Homo sapiens*. The 15 known human K_{2P} genes are placed into six subgroups; the amino acid percentage sequence identity is given for the subfamily members. The sequence identities were from ref 13.

subgroup, where TREK-1, TREK-2, and TRAAK share between 39.2% and 59.0% of sequence identity; in other subgroups such as TWIK and TALK the identity varies from 44.3% to 35.2%, respectively. The amino acid sequence conservation between K_{2P} subgroups is comparable to that between channels from other K^+ channel families such as K_v and K_{ir},[13] which allows us to witness the high conservation of these channels in nature.[25]

K_{2P} channels have been identified in plants, mammals, and other organisms. In plants, for instance, the genome of the model plant *Arabidopsis thaliana* includes five genes coding for K_{2P} channels named as tandem-pore K^+ channels TPK1−5 (*At*TPKs). Orthologues of *At*TPKs are found in all higher plants sequenced so far. In contrast, in algae, they have only been found in the chlorophyte *Ostreococcus*.[26] Although human K_{2P} channels and *At*TPKs share the same topology (2P/4TM), their sequence identities and similarities are low, varying between 5.9% and 18.9% for identity and 12.1% and 31.7% for similarity.[25] In this direction, our group previously studied the similarities and differences between K_{2P} channels in plants and animals regarding their physiology, as well as the nature of the last common ancestor (LCA) of these two groups of proteins. Through an extensive evolutionary analysis using bioinformatics we found that K_{2P} LCA was most likely a eukaryotic organism. Our findings showed that bioinformatics studies on K_{2P} channels (in mammals, plants, and other organisms) would allow understanding the evolution, molecular regulation mechanisms, and physiological modulation of these remarkable channels.[25]

Unfortunately, TASK channels 3D structures have not been resolved yet by X-ray crystallography or cryoelectron microscopy; however, the recent crystal release of other K_{2P} channels allowed us to describe the unique topology and structure of these channels and also to create models and understand how and why K_{2P} channels have different conformations in the membrane. Figure 2 illustrates the K_{2P}

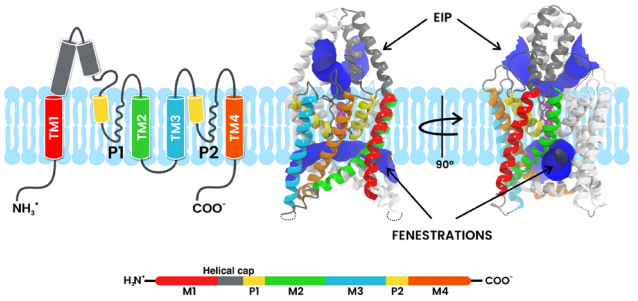

Figure 2. Architecture of K_{2P} channels. Topology and 3D structure of the human TWIK-1 channel. The blue surface represents the extracellular ion pathway (EIP) and side-fenestrations. TWIK-1 is rotated 90° for better representation.

channel topology. They have two-pore domains and four helical transmembrane segments per subunit (2P/4TM) and form dimers.[4] Nonetheless, heterodimers between K_{2P} channels such as TASK-1/TWIK-1[27] and TASK-1/-3[21,28−31] have been reported. In 2012, Miller and Long[12] and Brohawn et al.[13] deposited the first two K_{2P} channel crystals in the PDB database. They placed the 3D structure of TWIK-1 (PDB code 3UKM) and TRAAK (PDB code 3UM7), respectively. Those crystals revealed a unique cap structure formed by two large extracellular linkers from the M1 to the first pore loop (M1-P1 linker);[32] the cap forms two extracellular ion pathways (EIP) after the selectivity filter (Figure 2). Crystallized channels also display two open cavities facing the membrane known as side-fenestrations; these fenestrations are also present in other ion channels such as the voltage-gated sodium channels[33,34] and are one of the leading research topics in the field of rational drug design targeting hERG, sodium, and K_{2P} channels.[15,35−39] In 2013, Brohawn et al.[14] deposited another TRAAK crystal structure (PDB code 4I9W) but this time the TRAAK channel conformation was different, with one fenestration opened and the other one closed. This structure also revealed domain-swapped chain connectivity, where the TM4 helix interacting with the first pore domain (P1) of the same subunit of previous crystallographic structures now interacts with the first pore domain of the other subunit.

The physiological function of the cap is still poorly understood, and it remains unclear whether the cap and thus

DOI: 10.1021/acs.jmedchem.9b00248
J. Med. Chem. XXXX, XXX, XXX−XXX

K_{2P} channels assemble in two different conformations: domain-swapped or non-domain-swapped.[40] It is known that the presence of the extracellular cap confers resistance to K_{2P} channels against toxins,[13] conventional K^+ channel-blocking drugs such as tetraethylammonium (TEA), and 4-aminopyridine,[41] as well as polyunsaturated fatty acids.[12,42] Recently, we aimed at assessing whether there are structural differences between the K_{2P} channels that harbor a disulfide bridge in the extracellular cap[12,13,15,43,44] and those without it, such as TASK-1 and TASK-3. Functional alanine mutagenesis screening of TASK-1 along with homology modeling was used to build an experimentally validated model of the cap of disulfide-bridge free TASK-1 channels. The evidence presented suggests that the Cys residues at the tip of the cap structure in K_{2P} channels are not essential for channel assembly. It was proposed then that hydrophobic residues at the inner leaflets of the cap domains can interact with each other and that this way of stabilizing the cap is most likely conserved among K_{2P} channels.[32]

In 2014, Brohawn et al.[45] proposed a physical mechanism for the gating and mechanosensitivity of the human TRAAK channel. In these TRAAK crystal structures (PDB codes 4WFE, 4WFF, 4WFG, and 4WFH) the K^+ ion occupancy was associated with the conductance of the K_{2P} channels as well as the conformation of the side-fenestrations. Crystal structures where K^+ ions were found at the inner cavity have a closed side-fenestration; for this reason, the closed side-fenestration or "up state" was associated with the "conductive state", and the opened side-fenestration or "closed state" was associated with the "nonconductive state". In the conductive state, conformational changes in the M2, M3, and M4 transmembrane helices seal the side-fenestrations to prevent lipid access allowing the ion conduction through the channel. In 2013, Dong et al. deposited the structure of TREK-2 (PDB code 4BW5) with both fenestrations closed and the cap in a domain-swapped conformation.[15] In 2014, they deposited the crystal structure of TREK-1 (PDB code 4TWK) with the same conformation (both fenestrations closed and domain-swapped), and in 2015 the other three crystal structures of TREK-2 were deposited, all of them with the domain-swapped conformation and with both fenestrations opened (i) without ligand (PDB code 4XDJ), (ii) in complex with norfluoxetine (PDB code 4XDK), and (iii) in complex with brominated fluoxetine (PDB code 4XDL).[15] These last structures revealed insights into the binding site of the crystallized ligands and the role of the fenestrations in the binding mode and ion conductivity, since the conductive and nonconductive states of TREK-2 were also associated (as it was associated for TRAAK) with the ion occupancy at the selectivity filter. In this report, Dong et al. also studied the coordinated movement of all three involved helices (M2, M3, and M4) by molecular dynamics simulations (MDs). These simulations exhibited a downward movement of M2, M3, and M4 from the nonconductive state (side-fenestrations open) to adopt a conformation similar to the conductive state (side-fenestrations closed), thus indicating the occurrence of movements between the states. They described for the very first time (by crystal structures) the binding site of drugs such as norfluoxetine and brominated fluoxetine within a K_{2P} channel. These drugs bind within the side-fenestrations but do not bind into the inner cavity to directly block the ion path. The fenestrations provide a hydrophobic environment close to the selectivity filter in which both ligands promote the nonconductive state (open fenestrations).[15] In 2017, Lolicato et al.[46] obtained three crystallographic TREK-1 structures (PDB codes 6CQ6, 6CQ8, and 6CQ9) revealing a new binding site of small activators called "cryptic binding site". The cryptic pocket lies behind the selectivity filter where the binding of activators ML335 and ML402 is directly related to the regulation of a C-type-like inactivation gating.[46] These structures exhibit closed fenestrations consistent with Brohawn et al.[45] hypothesis stating that the "up state" is associated with a "conductive state." However, in 2014, the same group published crystal structures of two TRAAK channel mutants (G124I and W262S) gaining function and open fenestrations and providing contradicting results on gating regarding the Brohawn et al. hypothesis. In 2016, this contradiction was solved by McClenaghan et al.[47] When analyzing TREK-2 channels, they proposed that the K_{2P} channel gate is at the selectivity filter, as described by Schewe et al.[48] and that the filter can open independently from both the down and the up states. TREK2-G167I and TREK-W306S mutants, homologues to TRAAK-G124I and TRAAK-W262S mutants, respectively, directly activate the filter gate without closing fenestrations.

PHYSIOLOGICAL AND PATHOPHYSIOLOGICAL ROLE OF TASK CHANNELS

Some studies have shown that TASK channels are not involved in the regulation of breathing by hypercapnia in the brain stem.[49] However, TASK-1 (not TASK-3) channels may be involved in hypoxic ventilatory driven by the carotid bodies,[50] playing a role in sensing acidosis and hypoxia in glomus cells.[51] Both channels play an essential role in the central nervous system, in the cardiovascular system,[4] and in the regulation of the immune system.[52] The adrenal gland is also a significant site for TASK-1 and TASK-3 expression in both rodents and humans. TASK-1 null mice (TASK-$1^{-/-}$) show hyperaldosteronism, a pathological condition where an excess of aldosterone is produced by the adrenal gland.[53] TASK-1 and TASK-3 channels are also relevant for neuronal excitability, confirmed by the fact that TASK knockout mice are resistant to the hypnotic and immobilizing effects of halothane.[54] Both channels are activated by this volatile anesthetic.[55] Besides, TASK-$3^{-/-}$ mice exhibit pronounced sleep disorders and a marked reduction in the sensitivity to the halothane hypnotic effects.[56]

TASK-1 is present in many different tissues (pancreas, placenta, kidney, lung, liver, ovary, prostate, and small intestine) contributing to maintain the resting membrane potential.[57] This modulation appears to be important in some physiological contexts, including the transmission and anesthetic regulation of neuronal activity.[55] Strikingly, loss-of-function mutations in TASK-1 (*KCNK3*) cause pulmonary arterial hypertension (PAH).[58] However, it currently remains unclear whether TASK-1 inhibition, by drug-targeting this channel, will cause PAH side effects in animal model or humans.[59,60] TASK-1 was identified as a built-in rheostat negatively regulating thermogenesis, antagonizing norepinephrine-induced membrane depolarization by promoting K^+ efflux in brown adipocytes.[61]

TASK channels have been implicated in apoptosis and tumorigenicity.[62,63] TASK-3 has also brought considerable attention as a channel involved in carcinogenesis and tumor progression. TASK-3 was verified as an effective oncogene; its overexpression accelerates breast tumor formation and confers

DOI: 10.1021/acs.jmedchem.9b00248
J. Med. Chem. XXXX, XXX, XXX−XXX

Table 1. Principal Human TASK Channels Modulators

		activity				
no.	compound	% inhibition	IC_{50} (μM)	target	cell line	ref
1	A1899		0.035 ± 0.003	TASK-1[c]	X. oocytes	
			0.318 ± 0.030	TASK-3[c]		
			0.007 ± 0.001	TASK-1[d]	CHO cells	17
			0.070 ± 0.009	TASK-3[d]		
			12.0 ± 2.2	TASK-2[d]	X. oocytes	
			8.1 ± 2.3	TASK-4[d]		
			0.036	TASK-3*[f]	(FRT) epithelial cells	19
			1.6			98
2	A293		0.222 ± 0.038	TASK-1[c]	X. oocytes	93
			0.95 ± 0.1	TASK-3[c]		
			0.22	TASK-1[c]		69
3	alphaxolone	100 μM → 49.2 ± 6.2%		TASK-3[a]	X. oocytes	79
4	anandamide		3	TASK-1[a]	COS-7 cells	82
5	AVE0118		0.6	TASK-1[c]	X. oocytes	69
6	(±)-octoclothepin maleate		73.8 ± 20.4	TASK-3[g]	HEK293 cells	97
	Ba	100 μM → 11.0 ± 5.0%		TASK-3[a]	X. oocytes	79
7	bupivacaine	100 μM → 50.2 ± 10.9%		TASK-3[a]	X. oocytes	79
		100 μM → 56 ± 13%		TASK-3*[b]	COS-7 cells	24
			41 ± 10	TASK-1[c]	X. oocytes	88
	Cs^+	1 mM → 7.7 ± 7.6%↑		TASK-3[a]	X. oocytes	79
8	diethyl ether	0.6 mM → ≈40%		TASK-1[a]	COS cells	84
9	dihydro-β-erythroidine hydrobromide		73.8 ± 20.4	TASK-3[g]	HEK293 cells	97
	dihydropyrrolo[2,1-*a*]isoquinolines				X. oocytes	95
10	**1**		189.2 ± 27.0	TASK-3[c]		
11	**2**		96.7 ± 6.9	TASK-1[c]		
12	**3**		268.1 ± 47.4	TASK-3[c]		
13	**3**		83.5 ± 8.7	TASK-1[c]		
14	doxapram		0.41	TASK-1*[c]	X. oocytes	96
			37	TASK-3*[c]		
			16	TASK-3*[f]	(FRT) epithelial cells	18
			22			72
15	etidocaine		39 ± 9	TASK-1[c]	X. oocytes	88
16	glibenclamide	100 μM → 3.6 ± 2.7%		TASK-3[a]	X. oocytes	79
17	GW2974		50.1 ± 41.8	TASK-3[g]	HEK293 cells	97
18	halothane	1 mM → 65.6 ± 15.2%↑		TASK-3[a]	X. oocytes	79
		1 mM → ≈60%↑		TASK-1[a]	COS cells	84
19	ICAGEN-4		1.05	TASK-1[c]	X. oocytes	17
20	isoflurane	2 mM → ≈25%↑		TASK-1[a]	COS cells	84
21	ketamine	100 μM → 7.3 ± 2.2%		TASK-3[a]	X. oocytes	79
22	L-703,606 oxalate		45.5 ± 337	TASK-3[g]	HEK293 cells	97
23	lidocaine		222 ± 46	TASK-1[c]	X. oocytes	88
		1 mM → 62 ± 9%		TASK-3*[b]	COS-7 cells	24
24	loratadine		63.4 ± 39.6	TASK-3[g]	HEK293 cells	97
25	mepivacaine		709 ± 190	TASK-1[c]	X. oocytes	88
26	methanandamide		0.1	TASK-1[a]	COS-7 cells	82
27	mevastatin		159 ± 154	TASK-3[g]	HEK293 cells	97
28	mibefradil dihydrochloride		24.6 ± 217	TASK-3[g]	HEK293 cells	97
29	ML308		0,413	TASK-3[c]	HEK293 cells	94
			3.2	TASK-1[c]		
30	ML365		0.016	TASK-1[e]	CHO cells	99
			0.99	TASK-3[e]		
31	MSD-D		0.35	TASK-1[c]	X. oocytes	17
32	NPBA	10 μM → ≈6-fold↑		TASK-3[g]	CHO-K1	86
33	oligomycin A		47.7 ± 6.77	TASK-3[g]	HEK293 cells	97
34	pentobarbital	100 μM → 4.3 ± 2.6%		TASK-3[a]	X. oocytes	79
35	quinidine	100 μM → 42.2 ± 10.4%		TASK-3[a]	X. oocytes	79
		100 μM → 37 ± 6%		TASK-3*[b]	COS-7 cells	24
36	quinine	100 μM → 36.9 ± 6.9%		TASK-3[a]	X. oocytes	79
		100 μM → <20		TASK-1[c]	X. oocytes	21

DOI: 10.1021/acs.jmedchem.9b00248
J. Med. Chem. XXXX, XXX, XXX−XXX

Table 1. continued

no.	compound	activity		target	cell line	ref
		% inhibition	IC_{50} (μM)			
37	ropivacaine					
	R		51 ± 13	TASK-1[c]	X. oocytes	88
	S		53 ± 15	TASK-1[c]		
38	S9947		0.2	TASK-1[c]	X. oocytes	17
39	TEA	1 μM → 6.1 ± 3.3%		TASK-3[a]	X. oocytes	79
40	terbinafine	1 μM → 30%↑		TASK-3[a]	tsA201 cells	100
41	tetracaine		668 ± 214	TASK-1[c]	X. oocytes	88
	THPP series		(0.035 ± 0.005 to >100)	TASK-3[e]	HEK293 cells	18
			(0.19 ± 0.02 to 0.96 ± 0.02)	TASK-1[e]		
42	PK-THPP (**23**)		0.035 ± 0.005	TASK-3[e]		18
			0.30 ± 0.02	TASK-1[e]		
			0.01	TASK-3*[f]	(FRT) epithelial cells	18
			0.042			72
			0.243 ± 0.02	TASK-3[c]	X. oocytes	75
43	Zn	100 μM → 11 ± 4%		TASK-1[c]	TsA-201 cells	92
		100 μM → 87 ± 2%		TASK-3[c]		

[a]Whole cell patch clamp. [b]Outside-out patches. [c]Whole cell voltage clamp. [d]Inside-out macropatches. [e]Qpatch HT platform. [f]Using Chamber. [g]Ti^+ flux assay. ↑Activity increase. *Rat orthologues

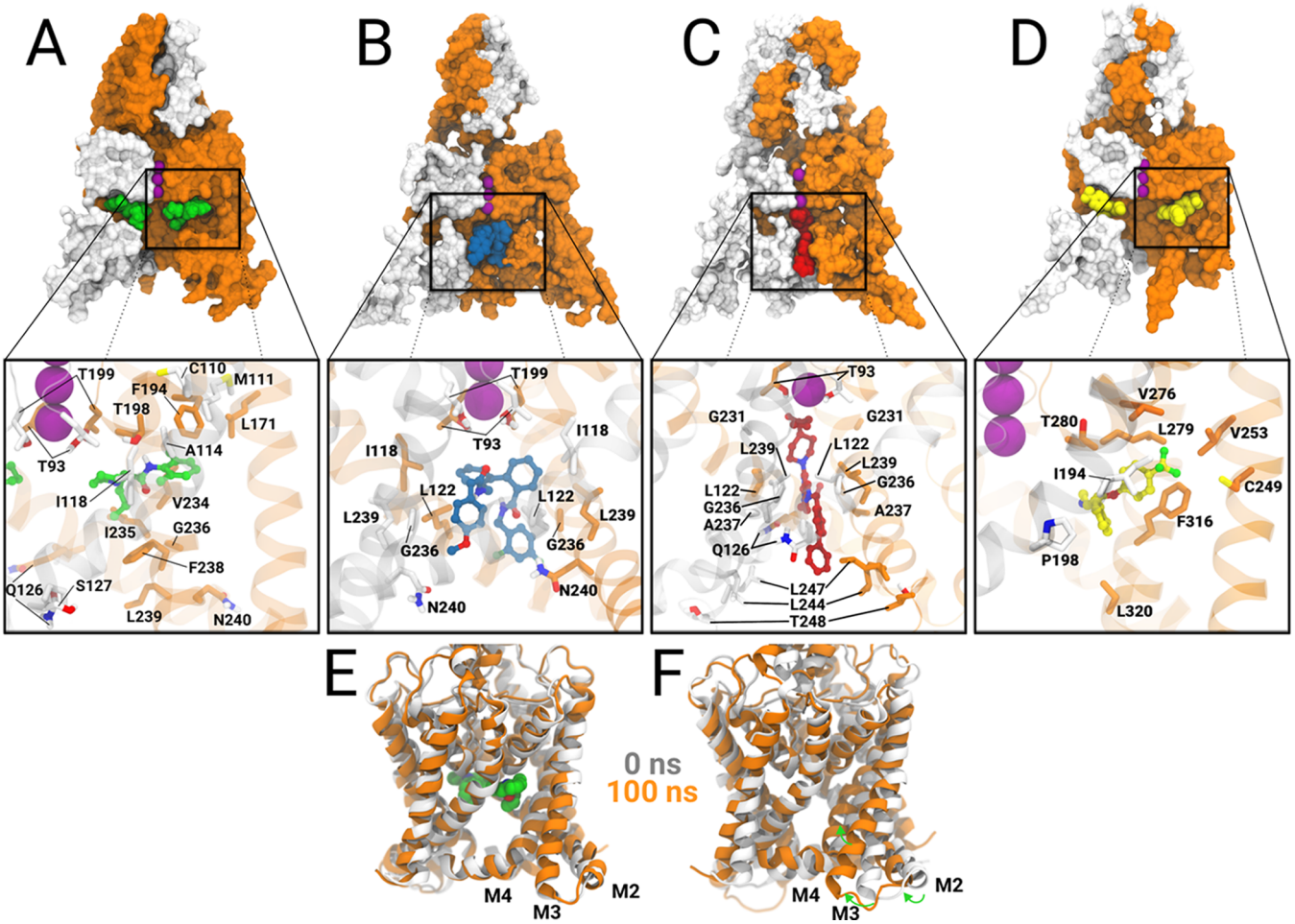

Figure 3. K_{2P} channels known binding sites. (A, B) Bupivacaine and A1899 binding sites in TASK-1 channels. (C) PK-THPP binding site in TASK-3. All interaction modes were described by functional mutagenesis screening and molecular dynamics simulations. (D) Norfluoxetine binding site in TREK-2 channels described by crystallographic structures. (E) TASK-1 in complex with bupivacaine (green) at lateral fenestrations before (gray) and after (orange) 100 ns of molecular dynamics simulations, illustrating how the drug prevents the "down" to "up" transition due the concerted movement of the M2, M3, and M4 transmembrane segments. (F) TASK-1 in the absence of bupivacaine before (gray) and after 100 ns (orange). Green arrows indicate the concerted movement of M2, M3, and M4 transmembrane segments causing the closure of lateral fenestrations.

DOI: 10.1021/acs.jmedchem.9b00248
J. Med. Chem. XXXX, XXX, XXX−XXX

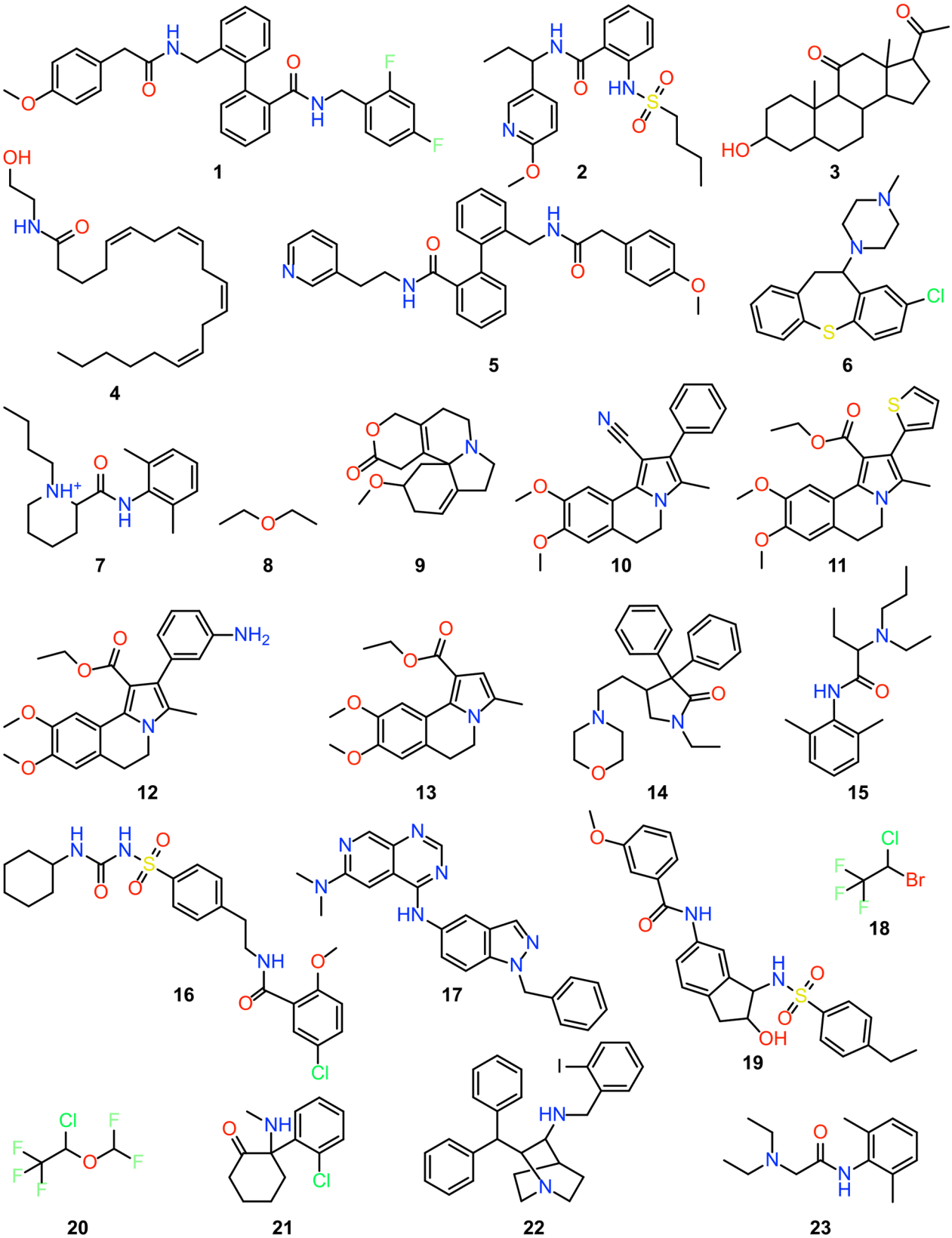

Figure 4. continued

DOI: 10.1021/acs.jmedchem.9b00248
J. Med. Chem. XXXX, XXX, XXX−XXX

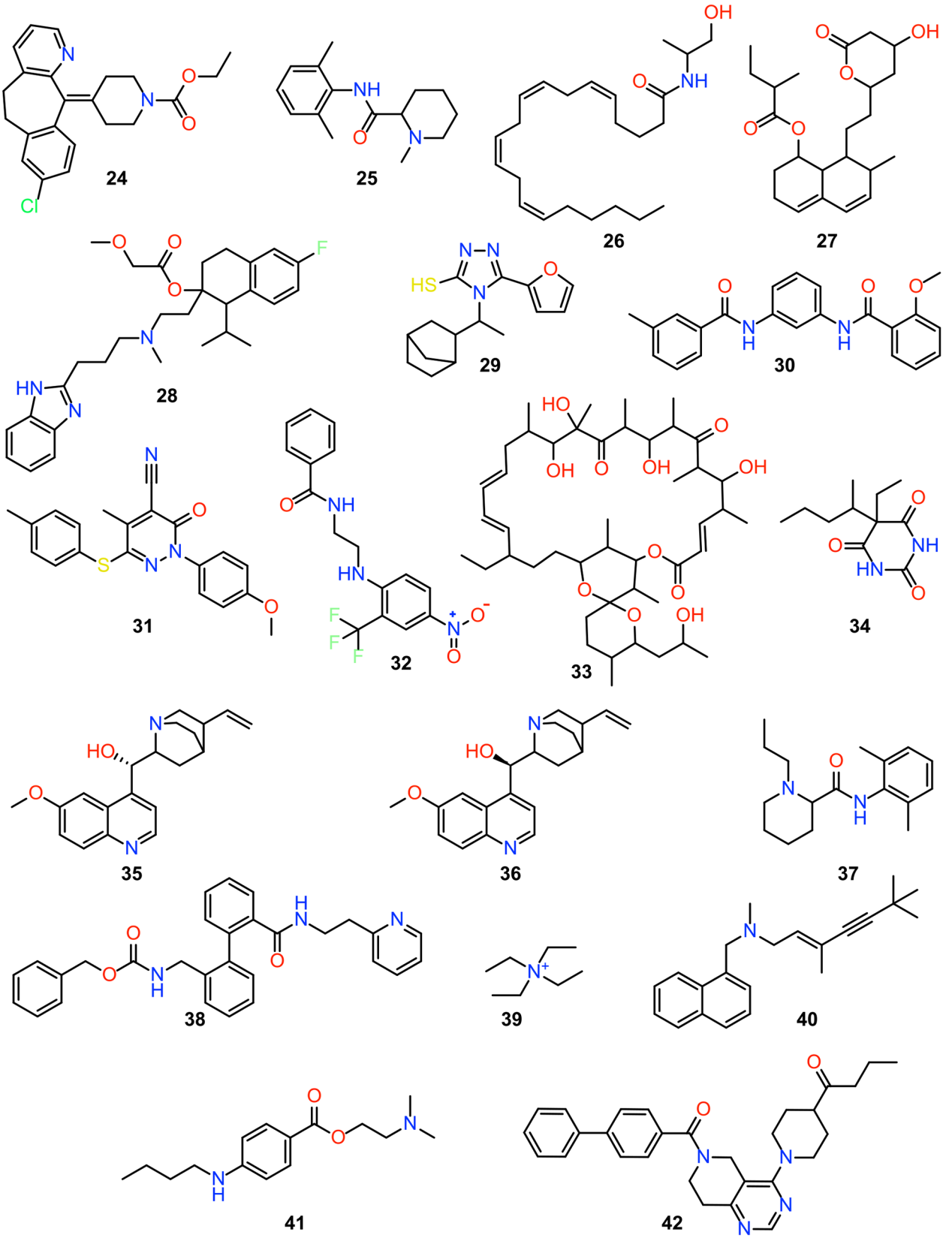

Figure 4. TASK modulators.

resistance to both hypoxia and serum deprivation.[62] Point mutations abolishing TASK-3 channel activity abrogate these

DOI: 10.1021/acs.jmedchem.9b00248
J. Med. Chem. XXXX, XXX, XXX−XXX

oncogenic functions,[64,65] and TASK-3 blockers caused a significant reduction in cell proliferation and an apoptosis increase in ovarian cancer cell lines.[66]

TASK BLOCK MECHANISM AND BIOPHYSICAL CHARACTERISTICS

TASK channels evolved as promising drug targets against atrial fibrillation,[67−70] sleep apnea,[69] diabetes,[71] pulmonary hypertension,[72] and cardiac conduction disorders.[73] Thus, there is a high medical need for specific TASK channel blockers or activators. As for other potassium channels, K_{2P} channel blockers described so far preferentially bind to a conserved binding site located in the central cavity. Thus, the TASK-1 inhibiting compounds A1899[17] and A293[74] are classical open channel blockers binding to the central cavity of channels (Table 1).

We recently found that the local anesthetic bupivacaine causes a voltage dependent block of TASK-1 and TASK-3 channels[35] (Figure 3A). This feature was not previously observed for any other TASK blocker described so far, such as A1899[17,36] and PK-THPP;[75] both blockers were found interacting in the central cavity (Figure 3B,C). For this reason, we subsequently mapped the bupivacaine binding site, using a functional alanine mutagenesis scan approach combined with molecular modeling experiments, and identified a novel allosteric binding site in the lateral fenestrations of TASK-1[35] (Figure 3A). Most importantly, bupivacaine is positioned too far lateral in the fenestrations to cause a classical open channel block by preventing K^+ passage through the central cavity. Thus, the drug uses a novel allosteric mechanism to cause a voltage dependent inhibition, which is specific to TASK-1 and TASK-3 but not for other K_{2P} channels tested.[35] We described that TASK-1 channels convert from the down to the up state during molecular dynamics simulations (MDs) which causes the putative TASK-1 side-fenestrations to close.[35] However, this conversion did not occur in the presence of the drug (Figure 3E,F). A similar conversion was also described for TWIK-1 by MDs,[37] where the movement of the transmembrane segments to open the fenestrations creates a hydrophobic barrier deep within the inner pore restricting full hydration of the inner cavity and, therefore, generating an energetic barrier limiting ion permeation.[76] Using MDs, Dong et al. also described how TREK-2 converts from the down to up state after 200 ns MDs and reported the norfluoxetine binding site at the fenestrations (Figure 3D).[15] In 2018, Brennecke and de Groot described by MDs how the TREK-2 up state (with the fenestration closed) stabilizes the selectivity filter, leading to a more conductive channel as compared to the down-state.[77] Nevertheless, it remains unknown whether TASK-1 channels gate in a comparable way as members of the TREK/TRAAK subfamily of K_{2P} channels and whether they physiologically convert into an "up"-state-like conformation. Thus, it also remains an open question whether the effects of bupivacaine on the state of fenestrations contribute to the mechanism of voltage-dependent inhibition.[35]

In TASK-1 homology models, the conversion to the up-state was avoided when bupivacaine was located in the binding site of the fenestrations. The transition is caused (like in other K_{2P} channels describe above) by a coordinated movement of M2, M3, and M4 helices (Figure 3E,F). These findings might lead to the hypotheses that the fenestration gating might be similar in all K_{2P} channels. However, the allosteric inhibition of bupivacaine in TASK-1 and TASK-3 channels (discussed above) suggests that these channels might gate in a different manner.[35]

K_{2P} channels were recently described to operate as K^+-activated potassium channels, in a way that K^+ ions can sense the voltage, causing a voltage-dependent K^+-efflux that removes a C-type-like inactivation of the selectivity filter.[48] Schewe et al. proposed a model in which the selectivity filter of K_{2P} channels acts as a one-way check valve, unidirectionally opened by potassium efflux.[48] Strikingly, we found that bupivacaine allosterically prevents this voltage-dependent K^+ flux gating in TASK-1 channels leading to a voltage dependent block. The fact that bupivacaine causes a voltage-dependent inhibition exclusively to TASK-1 and TASK-3 channels suggests that these channels might gate in a different manner.[35] This is also supported in literature, since for TASK channels it was not possible to determine a value in inside-out patches for the voltage of half-maximal activation[48] and Rb^+ did not strongly activate the channels but inhibited them.[48] On the other hand, and maybe even more straightforward as an explanation, the TASK-1/3 channel subtype specificity of the voltage-dependent inhibition might simply result from a specific set of amino acids determining a binding site exclusively located in the lateral fenestrations of TASK-1 and TASK-3.

Although local anesthetics are notoriously promiscuous and only show a low affinity block of TASK-1/3 channels, the new allosteric block mechanism might provide the molecular basis to develop highly potent subtype specific K_{2P} channel blockers with specific biophysical characteristics.

PHARMACOLOGY OF TASK CHANNELS

The pharmacology of TASK channels has been poorly studied over the past years. Here, we compile the TASK modulators reported in recent years (Table 1, Figure 4). TASK channels are insensitive to typical K^+ channel blockers such as Cs^+, tetraethylammonium (TEA), and 4-aminopyridine (4-AP).[78,79] Several molecules regulate these channels as neurotransmitters,[80] hormones,[78] alkaloids,[81] cannabinoids,[82] divalent cations,[83] and volatile anesthetics such as halothane and isoflurane;[84] none of these compounds are selective for TASK channels. TASK channels are stimulated by halothane at the C-terminal region, where 0.1−1.0 mM halothane increases more than 60% the TASK-1 channel activity and 1.0 mM halothane increases 66% the TASK-3 channel activity.[79,84] TASK-3 channels are also stimulated by other general anesthetics (halogenated agents) such as 2,2,2-tribromoethanol, 2,2,2-trichloroethanol, carbon tetrabromide, and carbon tetrachloride.[85] Recently, Tian et al. described that *N*-(2-((4-nitro-2-(trifluoromethyl)phenyl)amino)ethyl)benzamide (NPBA) activates TASK-3 channels by interacting with two distant clusters of residues, one located at the extracellular end of TM2 and the other cluster at the intracellular end of TM3.[86]

Regarding the study of the K_{2P} channels blockage, several authors have studied the effect of local anesthetics such as lidocaine and bupivacaine in K_{2P} channels such as TASK, TREK, and TALK.[4,18,19,87−90] Lidocaine poorly inhibits TASK channels ($IC_{50} \approx 220\ \mu M$),[18] and bupivacaine presumably binds TASK-1 channels at the side-fenestrations,[35] making it a perfect candidate to study the fenestrations role in the modulation of TASK. Bupivacaine is a voltage-dependent blocker inhibiting *r*TASK-1 ($IC_{50} = 41−68\ \mu M$) and *r*TASK-3 ($IC_{50} \approx 100\ \mu M$) channels.[6,88,91]

DOI: 10.1021/acs.jmedchem.9b00248
J. Med. Chem. XXXX, XXX, XXX−XXX

Other molecules can also bind TASK channels at the extracellular ion pathway (EIP) (Figure 2) such as Zn^{2+} and ruthenium red (RR). Zn^{2+} selectively blocks TASK-3 under physiological conditions by binding the residues His98 and Glu70.[92] The inhibition of TASK-3 by Zn^{2+}, just as pH_o gating, is cooperative and strongly impeded by increasing the extracellular K^+ concentration. Molecular dynamics simulations suggest that two Zn^{2+} ions might plausibly bind at sites defined by neutral His98 side chains flipped upward into the EIP at both sides of the pore entrance. Blockade of TASK-3 by Zn^{2+} and RR is K^+-dependent and shows virtual voltage independence, as expected from the interaction with superficial sites at the selectivity filter. Both Glu70 and His98 are proposed to form the blocker-binding site. Additionally, it is also possible that Glu70 side chain favors the blockers interaction by electrostatically increasing their local concentration.[44]

In recent studies, organic compounds such as A293,[93] A1899,[17] ML308,[94] and pyrido[4,3-*d*]pyrimidine derivatives[18] selectively inhibit TASK-1 and TASK-3 channels. Recently, Noriega-Navarro et al.[95] reported the application of dihydropyrrolo[2,1-*a*]isoquinoline derivatives (DPIs) as novel TASK inhibitors. Doxapram, on the other hand, blocks *r*TASK-1 with IC_{50} = 0.4 μM [96] and *r*TASK-3 with IC_{50} = 37 μM.[96] In addition, Bruner et al. described several compounds presenting inhibitory activity against TASK-3, such as loratadine (IC_{50} = 63.4 μM), mibefradil (IC_{50} = 24.6 μM), oligomicine A (IC_{50} = 47.7 μM), octoclothepin (IC_{50} = 73.8 μM), L-703,606 oxalate (IC_{50} = 45.5 μM), mevastatin (IC_{50} = 159 μM), dihydro-β-erythroidine (IC_{50} = 73.8 μM), and GW2974 (IC_{50} = 50.1 μM).[97] All these small compounds present physicochemical similarities (Figure 4) such as notable presence of aromatic rings, hydrogen-bond acceptors, and hydrophobic groups. These last groups are very important since their central cavity and side-fenestrations binding pockets are mostly hydrophobic.[17,35,36,69] We discussed below how the common physicochemical characteristics along these molecules allow them to interact with TASK channels.

Previous studies completed by our groups using computational and electrophysiological approaches showed that some known aromatic K_v1.5 blockers studied by the pharmaceutical industry (Sanofi-Aventis GmbH, patent WO2007/124849) are more effective against TASK-1 than K_v1.5 channels.[69] The inhibition of TASK-1 and K_v1.5 is caused by drug binding to the lipophilic residues facing the central cavity. Despite the physicochemical and sterically similarities in both drug binding sites, there are well-defined differences in their geometry, primarily arising from the dimeric structure of TASK-1 versus the 4-fold symmetry of Kv1.5 channel.[69] The most efficient aromatic K_v1.5 blocker in TASK-1 is A1899 since it is 68-fold more effective on TASK-1 than on K_v1.5,[69] blocking TASK-1 channel expressed in CHO cells with IC_{50} = 7 nM;[17] while A1899 blocks TASK-3 channel with IC_{50} = 70 nM. The binding site of A1899 in TASK channels was already identified; the only difference between TASK-1 and TASK-3 is a Met247 residue since TASK-3 has a leucine in this position.[17] In 2017 our group demonstrated by computational methods that A1899 is not facing the central cavity entirely and saw the relevance of the side fenestrations for the drug binding. It was proposed that A1899 binding at the inner cavity (Figure 3B) may provide an energetically favored conformation for the closed state of the channel.[36] In 2012, Coburn et al. described the a 5,6,7,8- tetrahydropyrido[4,3-*d*]pyrimidine (THPP) series as novel TASK-3 antagonist.[18] From that series, the compound PK-THPP was presented as the most potent TASK-3 blocker (IC_{50} = 35 nM). By molecular docking and site-directed mutation screening, it was proposed that PK-THPP, A1899, and doxapram bind in the central cavity of TASK-3 with the residues Leu122, Gly236, and Leu239.[19] We recently redefined the PK-THPP binding site into TASK-3 by alanine mutagenesis and molecular simulations and found that the residues Thr93, Gln126, Gly231, Ala237, Leu244, Leu247, and Thr248 are also part of the binding side at the central cavity (Figure 3C), along with the residues Leu122, Gly236, and Leu239 previously described.[75] In this sense, the use of fused heterocyclic compounds attracted the attention as new TASK blockers. Therefore, it is necessary for the development of more straightforward theoretical/experimental methodologies to find new heterocyclic derivatives with potential applications as TASK modulators.

CHALLENGES AND FUTURE DIRECTIONS

Ion channels play fundamental roles in several cellular functions and are involved in numerous pathologies underlying various diseases. Consequently, they constitute an "attractive" target with a substantial potential for drug discovery for a large number of diseases. However, despite their potential, some ion channel families such as K_{2P} channels are still scientifically and economically poorly exploited, and despite the considerable investment in ion channel screening, the need for developing potent K_{2P} channel modulators is yet to be achieved. There are multiples challenges to address, such as the use of alternative screening approaches like the phenotypic screen, since it is known that the use of pore-forming subunits expressed in heterologous cell system does not adequately represent how a cell may behave under a specific disease condition.[11,101−103] We could appreciate that ion channels are only one component of various signaling complexes involving accessory subunits, cofactors, enzymes, and other proteins involved in the transport at the cellular membrane level.[104,105] The evidence now shows that the pharmacology of a given ion channel can be strongly affected by the proteins associated with this channel in the cell.[106] New and innovative systems have been developed to overcome these problems, including two cell lines that can develop themselves into any somatic cell type: embryonic stem cells and induced pluripotent stem cells. Those cell lines are marking a new era with potential applications in drug design targeting ion channels.[107,108]

Other challenges to face regarding ion channels drug design are the poor chemical diversity available in databases; additionally, screening combinatorial libraries of small molecules could lead to difficulties since some moieties may interact with several different target molecules, raising the "selectivity" challenge. Here is when evolution tools are used by scientists since natural products such as toxins have been optimized by nature after millions of years for a phenotypic effect, and as a consequence of the evolution, natural products such as toxins can now eliminate target promiscuity and enrich their potency at the primary target. This growth makes them profitable for the design of pharmaceuticals targeting ion channels, enhanced by the multidisciplinary research between disciplines which are not traditionally linked to the ion channel drug discovery.[109−112] Another promising approach is the use of functional antibodies against ion channels, such as the use of monoclonal antibodies targeting nicotinic ion channels.[65,113,114]

DOI: 10.1021/acs.jmedchem.9b00248
J. Med. Chem. XXXX, XXX, XXX−XXX

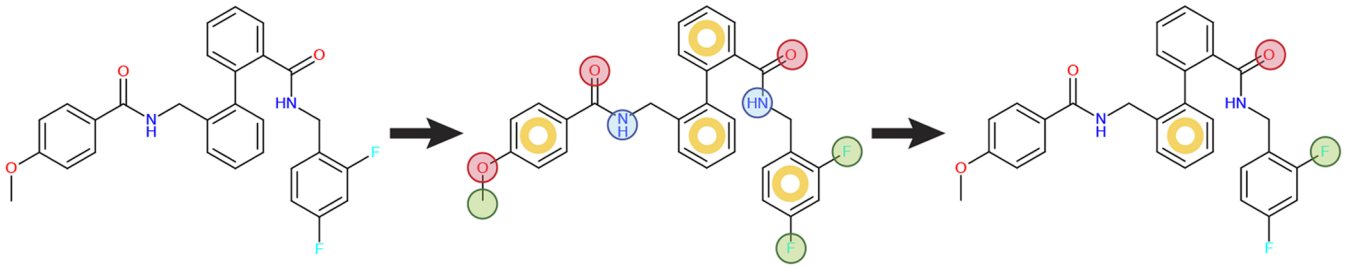

Figure 5. A common pharmacophore of TASK blockers. As an example, we show the selective TASK blocker A1899. To generate the TASK pharmacophore model, we first generated the 3D structures of all blockers and minimized the energy. The 2D structure of A1899 is displayed for better representation (left). Then, the pharmacophoric features are mapped in all blockers (central), and finally we generated a pharmacophore model by finding the common pharmacophoric features between ligands (right). Features are the following: H-bond acceptor (red), H-bond donor (blue), hydrophobic (green), and aromatic ring (orange).

One of the most significant advances in the rational drug design is the development of new computational methods and algorithms to study protein−ligand interactions and to predict if a given ligand will have activity against a specific target.[115] Among the most used methods, we can find molecular docking, molecular dynamics simulations, binding free energy calculations, and de novo drug design.[115] All those methods are based on the structure of the target, the ligand, or both and are usually combined with structure-based drug design (SBDD) strategies. The SBDD is most potent when it belongs to an entire drug lead discovery process, where the structure information has one of the greatest impacts on drug-discovery programs, improving the potency and selectivity of a lead molecule. Structural data are also employed in the design of small-molecule data sets with higher binding potential against a particular target. Another computational method where the pharmacophoric characteristics of a given set of ligands with proven activity act against a common target is called pharmacophore modeling. This computational approach describes steric and electronic characteristics needed for the interaction between a drug series and its target. "The pharmacophore can be considered as the largest common denominator shared by a set of active molecules."[116] Methods such as protein structure-based or ligand-based pharmacophore modeling[117] were implemented in pharmacophore modeling. While the protein structure-based modeling needs the 3D structure of the target or the complex to extract the chemical features in the active site and its relations, the ligand-based modeling extracts this information from a set of known ligands with the specific interactions with the target. In this method, pharmacophoric descriptors (H-bond acceptors, H-bond donor, aromatic ring, hydrophobic moieties, negative, and positives residues) are mapped between all the given ligands to generate a pharmacophore model. This model might be used either to search in a database of molecules for possible hits[118] or to design de novo ligands.[119] This approach has been widely used in drug discovery targeting ion channels, such as the K_{2P} family, where pharmacophore modeling and other computational tools identified new blockers such as NC30 with activity against TREK-1 channels.[120] Other ion channels inhibitors, like GAL-021 (a BK modulator), were also synthesized by modifying moieties of the almitrine pharmacophore.[121]

Here we explore the pharmacology of TASK channels, and by reviewing the structures of the reported TASK modulators and its activity against TASK channels (Table 1, Figure 4), we constructed the common ligand-based pharmacophore model between TASK modulators. Briefly, the blockers with reported IC_{50} (Table 1) were sorted into two groups, TASK-1 (A1899, A293, AVE0118, doxapram, etidocaine, ICAGEN-4, ML308, ML365, MSD-D, SS9947, and PK-THPP) and TASK-3 (A1899, A293, dihydro-β-erythroidine, doxapram, GW2974, L-703.606, loratadine, mevastatine, mibefradil, ML308, ML365, and oligomicine-A) blockers; we excluded bupivacaine since this drug has a known different binding site. The molecules were taken separately in each group for hypothesis generation using energy-optimized pharmacophore (e-pharmacophore). e-Pharmacophore is an approach to generate structure-based pharmacophores,[122] which uses a scoring function to accurately characterize protein−ligand interactions, resulting in improved database screening enrichments. Structures were sketched and processed using LigPrep with the force field OPLS-2005;[123] possible states of ionization at pH 7.0 ± 2.0 were generated with Epik. For both groups, the compounds were classified as active or inactive according to their IC_{50} (active, ≤20 μM; inactive, >20 μM).

Then, the pharmacophoric features were mapped for all the ligands in both groups with the software Phase,[124] using six pharmacophore features: hydrogen bond acceptor (A), hydrogen bond donor (D), hydrophobic group (H), negatively charged group (N), positively charged group (P), and aromatic ring (R). Each feature is defined by a set of SMARTS patterns (with the exception of the H and R features); then, the active and inactive ligands are defined randomly to develop the e-pharmacophore model. Stereochemical properties such as the isomerism were preserved according to data reported in the literature (Table 1). As expected, the same common pharmacophore (Figure 5) was identified for both TASK-1 and TASK-3 channels although the pharmacophore modeling was done in two different groups; this happens because the binding site in the central cavity only differs in the residue 247, where for TASK-1 is Met and for TASK-3 is Leu.[17]

One aromatic ring, one H-bond acceptor, and one hydrophobic group compose the identified TASK pharmacophore. This novel pharmacophore is common to all TASK blockers with IC_{50} < 20 μM. Unfortunately, there is not available information regarding TASK channels in complex with modulators from crystallographic structures to corroborate our findings. However, when comparing the TASK common pharmacophore reported here with the A1899 binding mode in TASK1 described by our group in 2017, we found that the carbonyl oxygen (H-bond acceptor in Figure 5) interacts with residues Gly236 and Arg240 located in the TASK-1 central cavity. Additionally, the aromatic ring interacts

DOI: 10.1021/acs.jmedchem.9b00248
J. Med. Chem. XXXX, XXX, XXX−XXX

with the Ile118 and Leu239, and the fluoride (hydrophobic feature) interacts with hydrophobic residues at the bottom of the TASK-1 pore.[36] These results allow us to hypothesize that active TASK blockers share common physicochemical and pharmacophoric features (Figure 5), allowing them to interact with TASK-1 and TASK-3 channels in a very similar way. On the other hand, we are aware that the three-point pharmacophore reported here is too general to guide the design of novel TASK modulators. However, it might be used as a molecular tool to understand the action mechanisms of different TASK channels modulators, such as other three-point pharmacophore models reported for K^+ channels modulators, like the common pharmacophore of different Kv1.5 blockers which preferentially inhibits TASK-1 channels,[69] or to describe a pharmacological master key mechanism that unlocks the selectivity filter gate in K^+ channels.[125] The ligand-based pharmacophore model reported here could also be used as a starting point to explore existing small-molecule databases, finding compounds with the same pharmacophoric characteristics as the presented model with potential activity against TASK channels. Thereby, the chemical space of molecules with potential activity against these channels could be expanded, enabling obtaining of new TASK channel modulators through combinatorial chemistry and lead optimization.

AUTHOR INFORMATION

Corresponding Author

*Telephone: (+56) 223036667. E-mail: david.ramirez@uautonoma.cl.

ORCID

Mauricio Bedoya: 0000-0002-3542-7528
Wendy González: 0000-0002-7535-6883
David Ramírez: 0000-0003-0002-1189

Author Contributions

The manuscript was written with contributions of all authors. All authors approved the final version of the manuscript.

Notes

The authors declare no competing financial interest.

Biographies

Mauricio Bedoya graduated from Pharmaceutical Chemistry at the Universidad de Antioquia of Medellín, Colombia. He is currently a graduate student in the Ph.D. program of Applied Sciences at the University of Talca, in Talca, Chile. His advisor is Dr. Wendy Gonzalez, Director of the Center of Bioinformatics and Molecular Simulation (CBSM) in the same institution. His thesis focuses on the ion conduction mechanism through the extracellular portals in the K_{2P} channels. Additionally, he has been studying new sites for allosteric inhibition in the same ion channels.

Susanne Rinné studied hospital and medicine technique, environmental technolgy, and biotechnology at the University of Applied Sciences in Giessen, Germany, and received her Ph.D. in Physiology at the Institute of Physiology and Pathophysiology in the group of Prof. Dr. Dr. J. Daut at the Philipps-University of Marburg, Germany. Subsequently she spent a postdoctoral fellowship in the laboratory of Prof. Dr. Dr. J. Daut before she joined in 2010 the group of Prof. Dr. N. Decher at the Philipps-University of Marburg, where she habilitated in 2018. Her research focuses on cardiac ion channels, particularly on K_{2P} channels, their regulation and pathophysiological relevance as well as their pharmacology.

Aytug K. Kiper studied human biology at the Philipps-University of Marburg, Germany, and received his Ph.D. in Physiology at the Institute of Physiology and Pathophysiology in Prof. Dr. Niels Decher's research group at the Philipps-University of Marburg, Germany. Subsequently he continued his research as postdoctoral fellow in Prof. Dr. Niels Decher's research group. His research focuses on cardiac ion channels. He is particularly interested in the structure, pharmacology, and pathophysiological relevance of K_{2P} channels.

Niels Decher received a Ph.D. in Pharmacy studying at the Johann-Wolfgang-Goethe University and the Aventis GmbH in Frankfurt, Germany, in 2002. Subsequently he spent a 2-year postdoctoral fellowship in the laboratory of Prof. Michael C. Sanguinetti at the University of Utah, U.S., before he joined in 2004 the group of Prof. Dr. Dr. Jürgen Daut at the Philipps-University of Marburg, Germany. In 2010 he was appointed as a Professor for Vegetative Physiology at the Philipps-University of Marburg. His research focuses on cardiac and neuronal ion channels and their pathophysiological relevance, pharmacology, and potential as drug targets for different diseases.

Wendy González received a Ph.D. in Sciences and focused on plant genetic engineering, studying at the University of Talca the structural and functional properties of plant Shaker potassium channels (2010). Subsequently she spent 2 years of postdoctoral fellowship in the laboratory of Prof. Dr. Ingo Dreyer at the University of Postdam, Germany, and at the end of 2012 she became the Director of the Center for Bioinformatics, Simulation and Modelling (CBSM) at the University of Talca. In 2014 she was appointed as Associate Professor at the University of Talca, and in 2017 she became co-researcher of the Millennium Nucleus of Ion Channels-Associated Diseases. The focus of her research is the molecular modeling of ion channels and the development of new drugs targeting ion channels for different diseases.

David Ramírez received his Ph.D. in Applied Sciences in early 2017 from the Center for Bioinformatics, Simulation and Modelling (CBSM) at the University of Talca in the laboratory of Dr. Wendy González. He spent 1 year of postdoctoral fellowship in the same group. Then, he joined the laboratory of Prof. Dr. José Argüello as a postdoctoral fellow at the Worcester Polytechnic Institute, U.S. In early 2019 he was appointed as Assistant Professor at the Institute of Biomedical Sciences at Universidad Autónoma de Chile. His research focuses on membrane proteins using both experimental and theoretical approaches, focusing on pharmacology and modulation of ion channels as well as transport mechanisms in plant and bacteria transporters.

ACKNOWLEDGMENTS

The authors express their sincere gratitude to M. A. Claudia Daza for assistance with manuscript editing. We thank the University of Talca for the doctoral scholarship of M.B. N.D. was supported by a grant of the Deutsche Forschungsgemeinschaft (Grant DE1482-4/1). W.G. was supported by the FONDECYT (Fondo Nacional de Desarrollo Cientifico y Tecnológico) Grant 1191133 and the Millennium Nucleus of Ion Channels Associated Diseases (MiNICAD) belonging to the Iniciativa Científica Milenio, Ministry of Economy, Development and Tourism, Chile. D.R. was supported by the FONDECYT Grant 11180604.

ABBREVIATIONS USED

aa, amino acids; CHO, Chinese hamster ovary; COS, cell lines derived from the CV-1 cells; EIP, extracellular ion pathway; FRT, Fischer rat thyroid; HEK, human embryonic kidney;

DOI: 10.1021/acs.jmedchem.9b00248
J. Med. Chem. XXXX, XXX, XXX−XXX

HRE, halothane response element; K_{2P}, two-pore domain K^+ channels; LCA, last common ancestor; MDs, molecular dynamics simulations; PDB, Protein Data Bank; P1, first pore domain; P2, second pore domain; RR, ruthenium red; SBDD, structure-based drug design; SF, selectivity filter; S1, S2, S3, and S4, ion occupancy sites 1, 2, 3, and 4, respectively; TEA, tetraethylammonium; THPP, 5,6,7,8-tetrahydropyrido-[4,3-*d*]pyrimidine; TM, transmembrane domain; TPK, tandem-pore K^+ channel; X. oocytes, *Xenopus laevis* oocytes

REFERENCES

(1) Vivier, D.; Bennis, K.; Lesage, F.; Ducki, S. Perspectives on the Two-Pore Domain Potassium Channel TREK-1 (TWIK-Related K^+ Channel 1). A Novel Therapeutic Target? *J. Med. Chem.* **2016**, *59* (11), 5149−5157.

(2) Bagal, S. K.; Brown, A. D.; Cox, P. J.; Omoto, K.; Owen, R. M.; Pryde, D. C.; Sidders, B.; Skerratt, S. E.; Stevens, E. B.; Storer, R. I.; et al. Ion Channels as Therapeutic Targets: A Drug Discovery Perspective. *J. Med. Chem.* **2013**, *56* (3), 593−624.

(3) Lesage, F. Pharmacology of Neuronal Background Potassium Channels. *Neuropharmacology* **2003**, *44* (1), 1−7.

(4) Goldstein, S. A. N.; Bockenhauer, D.; O'Kelly, I.; Zilberberg, N. Potassium Leak Channels and the KCNK Family of Two-p-Domain Subunits. *Nat. Rev. Neurosci.* **2001**, *2* (3), 175−184.

(5) Bayliss, D. A.; Barrett, P. Q. Emerging Roles for Two-Pore-Domain Potassium Channels and Their Potential Therapeutic Impact. *Trends Pharmacol. Sci.* **2008**, *29* (11), 566−575.

(6) Lotshaw, D. P. Biophysical, Pharmacological, and Functional Characteristics of Cloned and Native Mammalian Two-Pore Domain K^+ Channels. *Cell Biochem. Biophys.* **2007**, *47* (2), 209−256.

(7) Duprat, F.; Lauritzen, I.; Patel, A.; Honoré, E. The TASK Background K_{2P} Channels: Chemo- and Nutrient Sensors. *Trends Neurosci.* **2007**, *30* (11), 573−580.

(8) Karschin, C.; Wischmeyer, E.; Preisig-Müller, R.; Rajan, S.; Derst, C.; Grzeschik, K.-H.; Daut, J.; Karschin, A. Expression Pattern in Brain of TASK-1, TASK-3, and a Tandem Pore Domain K^+ Channel Subunit, TASK-5, Associated with the Central Auditory Nervous System. *Mol. Cell. Neurosci.* **2001**, *18* (6), 632−648.

(9) Bayliss, D. a; Sirois, J. E.; Talley, E. M. The TASK Family: Two-Pore Domain Background K^+ Channels. *Mol. Interventions* **2003**, *3* (4), 205−219.

(10) Patel, A. J.; Lazdunski, M. The 2P-Domain K^+ Channels: Role in Apoptosis and Tumorigenesis. *Pfluegers Arch.* **2004**, *448* (3), 261−273.

(11) Wickenden, A.; Priest, B.; Erdemli, G. Ion Channel Drug Discovery: Challenges and Future Directions. *Future Med. Chem.* **2012**, *4* (5), 661−679.

(12) Miller, A. N.; Long, S. B. Crystal Structure of the Human Two-Pore Domain Potassium Channel K2P1. *Science* **2012**, *335* (6067), 432−436.

(13) Brohawn, S. G.; del Mármol, J.; MacKinnon, R. Crystal Structure of the Human K2P TRAAK, a Lipid- and Mechano-Sensitive K^+ Ion Channel. *Science* **2012**, *335* (6067), 436−441.

(14) Brohawn, S. G.; Campbell, E. B.; MacKinnon, R. Domain-Swapped Chain Connectivity and Gated Membrane Access in a Fab-Mediated Crystal of the Human TRAAK K^+ Channel. *Proc. Natl. Acad. Sci. U. S. A.* **2013**, *110* (6), 2129−2134.

(15) Dong, Y. Y.; Pike, A. C. W.; Mackenzie, A.; McClenaghan, C.; Aryal, P.; Dong, L.; Quigley, A.; Grieben, M.; Goubin, S.; Mukhopadhyay, S.; et al. K2P Channel Gating Mechanisms Revealed by Structures of TREK-2 and a Complex with Prozac. *Science* **2015**, *347* (6227), 1256−1259.

(16) Brohawn, S. G.; Campbell, E. B.; MacKinnon, R. Physical Mechanism for Gating and Mechanosensitivity of the Human TRAAK K^+ Channel. *Nature* **2014**, *516* (7529), 126−130.

(17) Streit, A. K.; Netter, M. F.; Kempf, F.; Walecki, M.; Rinne, S.; Bollepalli, M. K.; Preisig-Muller, R.; Renigunta, V.; Daut, J.; Baukrowitz, T.; et al. A Specific Two-Pore Domain Potassium Channel Blocker Defines the Structure of the TASK-1 Open Pore. *J. Biol. Chem.* **2011**, *286* (16), 13977−13984.

(18) Coburn, C. a; Luo, Y.; Cui, M.; Wang, J.; Soll, R.; Dong, J.; Hu, B.; Lyon, M. a; Santarelli, V. P.; Kraus, R. L.; et al. Discovery of a Pharmacologically Active Antagonist of the Two-Pore-Domain Potassium Channel K_{2P}9.1 (TASK-3). *ChemMedChem* **2012**, *7* (1), 123−133.

(19) Chokshi, R. H.; Larsen, A. T.; Bhayana, B.; Cotten, J. F. Breathing Stimulant Compounds Inhibit TASK-3 Potassium Channel Function Likely by Binding at a Common Site in the Channel Pore. *Mol. Pharmacol.* **2015**, *88*, 926−934.

(20) Flaherty, D. P.; Simpson, D. S.; Miller, M.; Maki, B. E.; Zou, B.; Shi, J.; Wu, M.; McManus, O. B.; Aubé, J.; Li, M.; et al. Potent and Selective Inhibitors of the TASK-1 Potassium Channel through Chemical Optimization of a Bis-Amide Scaffold. *Bioorg. Med. Chem. Lett.* **2014**, *24* (16), 3968−3973.

(21) Duprat, F.; Lesage, F.; Fink, M.; Reyes, R.; Heurteaux, C.; Lazdunski, M. TASK, a Human Background K^+ Channel to Sense External pH Variations near Physiological PH. *EMBO J.* **1997**, *16* (17), 5464−5471.

(22) Rajan, S.; Wischmeyer, E.; Xin Liu, G.; Preisig-Müller, R.; Daut, J.; Karschin, A.; Derst, C. TASK-3, a Novel Tandem Pore Domain Acid-sensitive K+ Channel. An Extracellular Histidine as pH Sensor. *J. Biol. Chem.* **2000**, *275* (22), 16650−16657.

(23) Vega-Saenz de Miera, E.; Lau, D. H.; Zhadina, M.; Pountney, D.; Coetzee, W. A.; Rudy, B. KT3.2 and KT3.3, Two Novel Human Two-Pore K^+ Channels Closely Related to TASK-1. *J. Neurophysiol.* **2001**, *86* (1), 130−142.

(24) Kim, D.; Gnatenco, C. TASK-5, a New Member of the Tandem-Pore K^+ Channel Family. *Biochem. Biophys. Res. Commun.* **2001**, *284* (4), 923−930.

(25) González, W.; Valdebenito, B.; Caballero, J.; Riadi, G.; Riedelsberger, J.; Martínez, G.; Ramírez, D.; Zúñiga, L.; Sepúlveda, F. V.; Dreyer, I.; et al. K_{2P} Channels in Plants and Animals. *Pfluegers Arch.* **2015**, *467* (5), 1091−1104.

(26) Voelker, C.; Gomez-Porras, J. L.; Becker, D.; Hamamoto, S.; Uozumi, N.; Gambale, F.; Mueller-Roeber, B.; Czempinski, K.; Dreyer, I. Roles of Tandem-Pore K^+ Channels in Plants - A Puzzle Still To Be Solved. *Plant Biology*; Wiley Online Library, 2010; pp 56−63.

(27) Plant, L. D.; Zuniga, L.; Araki, D.; Marks, J. D.; Goldstein, S. A. N. SUMOylation Silences Heterodimeric TASK Potassium Channels Containing K2P1 Subunits in Cerebellar Granule Neurons. *Sci. Signaling* **2012**, *5* (251), ra84.

(28) Kang, D.; Han, J.; Talley, E. M.; Bayliss, D. A.; Kim, D. Functional Expression of TASK-1/TASK-3 Heteromers in Cerebellar Granule Cells. *J. Physiol.* **2004**, *554* (1), 64−77.

(29) Berg, A. P.; Talley, E. M.; Manger, J. P.; Bayliss, D. A. Motoneurons Express Heteromeric TWIK-Related Acid-Sensitive K^+ (TASK) Channels Containing TASK-1 (KCNK3) and TASK-3 (KCNK9) Subunits. *J. Neurosci.* **2004**, *24* (30), 6693−6702.

(30) Clarke, C. E.; Veale, E. L.; Green, P. J.; Meadows, H. J.; Mathie, A. Selective Block of the Human 2-P Domain Potassium Channel, TASK-3, and the Native Leak Potassium Current, IK_{SO}, by Zinc. *J. Physiol.* **2004**, *560* (1), 51−62.

(31) Czirják, G.; Enyedi, P. Formation of Functional Heterodimers between the TASK-1 and TASK-3 Two-Pore Domain Potassium Channel Subunits. *J. Biol. Chem.* **2002**, *277* (7), 5426−5432.

(32) Goldstein, M.; Rinné, S.; Kiper, A. K.; Ramírez, D.; Netter, M. F.; Bustos, D.; Ortiz-Bonnin, B.; González, W.; Decher, N. Functional Mutagenesis Screens Reveal the "Cap Structure" Formation in Disulfide-Bridge Free TASK Channels. *Sci. Rep.* **2016**, *6* (1), 19492.

(33) Kaczmarski, J. A.; Corry, B. Investigating the Size and Dynamics of Voltage-Gated Sodium Channel Fenestrations. A Molecular Dynamics Study. *Channels* **2014**, *8* (3), 264−277.

(34) Payandeh, J.; Gamal El-Din, T. M.; Scheuer, T.; Zheng, N.; Catterall, W. A. Crystal Structure of a Voltage-Gated Sodium Channel in Two Potentially Inactivated States. *Nature* **2012**, *486* (7401), 135−139.

DOI: 10.1021/acs.jmedchem.9b00248
J. Med. Chem. XXXX, XXX, XXX−XXX

(35) Rinné, S.; Kiper, A. K.; Vowinkel, K. S.; Ramírez, D.; Schewe, M.; Bedoya, M.; Aser, D.; Gensler, I.; Netter, M. F.; Stansfeld, P. J.; Baukrowitz, T.; Gonzalez, W.; Decher, N. The Molecular Basis for an Allosteric Inhibition of K^+-Flux Gating in K_{2P} Channels. *eLife* **2019**, *8*, e39476.
(36) Ramírez, D.; Arévalo, B.; Martínez, G.; Rinné, S.; Sepúlveda, F. V.; Decher, N.; González, W. Side Fenestrations Provide an "Anchor" for a Stable Binding of A1899 to the Pore of TASK-1 Potassium Channels. *Mol. Pharmaceutics* **2017**, *14* (7), 2197−2208.
(37) Jorgensen, C.; Darré, L.; Oakes, V.; Torella, R.; Pryde, D.; Domene, C. Lateral Fenestrations in K^+-Channels Explored Using Molecular Dynamics Simulations. *Mol. Pharmaceutics* **2016**, *13* (7), 2263−2273.
(38) Saxena, P.; Zangerl-Plessl, E. M.; Linder, T.; Windisch, A.; Hohaus, A.; Timin, E.; Hering, S.; Stary-Weinzinger, A. New Potential Binding Determinant for HERG Channel Inhibitors. *Sci. Rep.* **2016**, *6* (1), 24182.
(39) Buyan, A.; Sun, D.; Corry, B. Protonation State of Inhibitors Determines Interaction Sites within Voltage-Gated Sodium Channels. *Proc. Natl. Acad. Sci. U. S. A.* **2018**, *115* (14), E3135−E3144.
(40) Zúñiga, L.; Zúñiga, R. Understanding the Cap Structure in K2P Channels. *Front. Physiol.* **2016**, *7*, 1−5.
(41) Mathie, A.; Veale, E. L. Therapeutic Potential of Neuronal Two-Pore Domain Potassium-Channel Modulators. *Curr. Opin. Invest. Drugs* **2007**, *8* (7), 555−562.
(42) Fink, M.; Lesage, F.; Duprat, F.; Heurteaux, C.; Reyes, R.; Fosset, M.; Lazdunski, M. A Neuronal Two P Domain K^+ Channel Stimulated by Arachidonic Acid and Polyunsaturated Fatty Acids. *EMBO J.* **1998**, *17* (12), 3297−3308.
(43) Lesage, F.; Reyes, R.; Fink, M.; Duprat, F.; Guillemare, E.; Lazdunski, M. Dimerization of TWIK-1 K^+ Channel Subunits via a Disulfide Bridge. *EMBO J.* **1996**, *15* (23), 6400−6407.
(44) Gonzá lez, W.; Zúniga, L.; Cid, L. P.; Arévalo, B.; Niemeyer, M. I.; Sepúlveda, F. V. An Extracellular Ion Pathway Plays a Central Role in the Cooperative Gating of a K_{2P} K^+ Channel by Extracellular pH. *J. Biol. Chem.* **2013**, *288* (8), 5984−5991.
(45) Brohawn, S. G.; Su, Z.; MacKinnon, R. Mechanosensitivity Is Mediated Directly by the Lipid Membrane in TRAAK and TREK1 K^+ Channels. *Proc. Natl. Acad. Sci. U. S. A.* **2014**, *111* (9), 3614−3619.
(46) Lolicato, M.; Arrigoni, C.; Mori, T.; Sekioka, Y.; Bryant, C.; Clark, K. A.; Minor, D. L. K_{2P}2.1 (TREK-1)-Activator Complexes Reveal a Cryptic Selectivity Filter Binding Site. *Nature* **2017**, *547* (7663), 364−368.
(47) McClenaghan, C.; Schewe, M.; Aryal, P.; Carpenter, E. P.; Baukrowitz, T.; Tucker, S. J. Polymodal Activation of the TREK-2 K2P Channel Produces Structurally Distinct Open States. *J. Gen. Physiol.* **2016**, *147* (6), 497−505.
(48) Schewe, M.; Nematian-Ardestani, E.; Sun, H.; Musinszki, M.; Cordeiro, S.; Bucci, G.; de Groot, B. L.; Tucker, S. J.; Rapedius, M.; Baukrowitz, T. A Non-Canonical Voltage-Sensing Mechanism Controls Gating in K2P K^+ Channels. *Cell* **2016**, *164* (5), 937−949.
(49) Mulkey, D. K.; Talley, E. M.; Stornetta, R. L.; Siegel, A. R.; West, G. H.; Chen, X.; Sen, N.; Mistry, A. M.; Guyenet, P. G.; Bayliss, D. A. TASK Channels Determine pH Sensitivity in Select Respiratory Neurons But Do Not Contribute to Central Respiratory Chemosensitivity. *J. Neurosci.* **2007**, *27* (51), 14049−14058.
(50) Trapp, S.; Aller, M. I.; Wisden, W.; Gourine, A. V. A Role for TASK-1 (KCNK3) Channels in the Chemosensory Control of Breathing. *J. Neurosci.* **2008**, *28* (35), 8844−8850.
(51) Ortega-Sáenz, P.; Levitsky, K. L.; Marcos-Almaraz, M. T.; Bonilla-Henao, V.; Pascual, A.; López-Barneo, J. Carotid Body Chemosensory Responses in Mice Deficient of TASK Channels. *J. Gen. Physiol.* **2010**, *135* (4), 379−392.
(52) Meuth, S. G.; Bittner, S.; Meuth, P.; Simon, O. J.; Budde, T.; Wiendl, H. TWIK-Related Acid-Sensitive K^+ Channel 1 (TASK1) and TASK3 Critically Influence T Lymphocyte Effector Functions. *J. Biol. Chem.* **2008**, *283* (21), 14559−14570.
(53) Heitzmann, D.; Derand, R.; Jungbauer, S.; Bandulik, S.; Sterner, C.; Schweda, F.; El Wakil, A.; Lalli, E.; Guy, N.; Mengual, R.; et al. Invalidation of TASK1 Potassium Channels Disrupts Adrenal Gland Zonation and Mineralocorticoid Homeostasis. *EMBO J.* **2008**, *27* (1), 179−187.
(54) Lazarenko, R. M.; Willcox, S. C.; Shu, S.; Berg, A. P.; Jevtovic-Todorovic, V.; Talley, E. M.; Chen, X.; Bayliss, D. A. Motoneuronal TASK Channels Contribute to Immobilizing Effects of Inhalational General Anesthetics. *J. Neurosci.* **2010**, *30* (22), 7691−7704.
(55) Talley, E. M.; Bayliss, D. A. Modulation of TASK-1 (Kcnk3) and TASK-3 (Kcnk9) Potassium Channels. Volatile Anesthetics and Neurotransmitters Share a Molecular Site of Action. *J. Biol. Chem.* **2002**, *277* (20), 17733−17742.
(56) Pang, D. S. J.; Robledo, C. J.; Carr, D. R.; Gent, T. C.; Vyssotski, A. L.; Caley, A.; Zecharia, A. Y.; Wisden, W.; Brickley, S. G.; Franks, N. P. An Unexpected Role for TASK-3 Potassium Channels in Network Oscillations with Implications for Sleep Mechanisms and Anesthetic Action. *Proc. Natl. Acad. Sci. U. S. A.* **2009**, *106* (41), 17546−17551.
(57) Lesage, F.; Lazdunski, M. Molecular and Functional Properties of Two-Pore-Domain Potassium Channels. *Am. J. Physiol. Renal Physiol.* **2000**, *279* (5), F793−801.
(58) Ma, L.; Roman-Campos, D.; Austin, E. D.; Eyries, M.; Sampson, K. S.; Soubrier, F.; Germain, M.; Trégouët, D.-A.; Borczuk, A.; Rosenzweig, E. B.; et al. A Novel Channelopathy in Pulmonary Arterial Hypertension. *N. Engl. J. Med.* **2013**, *369* (4), 351−361.
(59) Olschewski, A.; Chandran, N.; Olschewski, H. Letter by Olschewski et al Regarding Article, "Upregulation of K_{2P}3.1 K^+ Current Causes Action Potential Shortening in Patients With Chronic Atrial Fibrillation.". *Circulation* **2016**, *133* (11), e439.
(60) Schmidt, C.; Wiedmann, F.; Voigt, N.; Zhou, X.-B.; Heijman, J.; Lang, S.; Albert, V.; Kallenberger, S.; Ruhparwar, A.; Szabó, G.; et al. Response to Letter Regarding Article, "Upregulation of K_{2P}3.1 K^+ Current Causes Action Potential Shortening in Patients With Chronic Atrial Fibrillation.". *Circulation* **2016**, *133* (11), e440−e441.
(61) Chen, Y.; Zeng, X.; Huang, X.; Serag, S.; Woolf, C. J.; Spiegelman, B. M. Crosstalk between KCNK3-Mediated Ion Current and Adrenergic Signaling Regulates Adipose Thermogenesis and Obesity. *Cell* **2017**, *171* (4), 836−848.
(62) Mu, D.; Chen, L.; Zhang, X.; See, L.-H.; Koch, C. M.; Yen, C.; Tong, J. J.; Spiegel, L.; Nguyen, K. C. Q.; Servoss, A.; et al. Genomic Amplification and Oncogenic Properties of the KCNK9 Potassium Channel Gene. *Cancer Cell* **2003**, *3* (3), 297−302.
(63) Williams, S.; Bateman, A.; O'Kelly, I. Altered Expression of Two-Pore Domain Potassium (K_{2P}) Channels in Cancer. *PLoS One* **2013**, *8* (10), e74589.
(64) Pei, L.; Wiser, O.; Slavin, A.; Mu, D.; Powers, S.; Jan, L. Y.; Hoey, T. Oncogenic Potential of TASK3 (Kcnk9) Depends on K^+ Channel Function. *Proc. Natl. Acad. Sci. U. S. A.* **2003**, *100* (13), 7803−7807.
(65) Sun, H.; Luo, L.; Lal, B.; Ma, X.; Chen, L.; Hann, C. L.; Fulton, A. M.; Leahy, D. J.; Laterra, J.; Li, M. A Monoclonal Antibody against KCNK9 K(+) Channel Extracellular Domain Inhibits Tumour Growth and Metastasis. *Nat. Commun.* **2016**, *7* (1), 10339.
(66) Innamaa, A.; Jackson, L.; Asher, V.; Van Shalkwyk, G.; Warren, A.; Hay, D.; Bali, A.; Sowter, H.; Khan, R. Expression and Prognostic Significance of the Oncogenic K2P Potassium Channel KCNK9 (TASK-3) in Ovarian Carcinoma. *Anticancer Res.* **2013**, *33* (4), 1401−1408.
(67) Limberg, S. H.; Netter, M. F.; Rolfes, C.; Rinné, S.; Schlichthörl, G.; Zuzarte, M.; Vassiliou, T.; Moosdorf, R.; Wulf, H.; Daut, J.; et al. TASK-1 Channels May Modulate Action Potential Duration of Human Atrial Cardiomyocytes. *Cell. Physiol. Biochem.* **2011**, *28* (4), 613−624.
(68) Liang, B.; Soka, M.; Christensen, A. H.; Olesen, M. S.; Larsen, A. P.; Knop, F. K.; Wang, F.; Nielsen, J. B.; Andersen, M. N.; Humphreys, D.; et al. Genetic Variation in the Two-Pore Domain Potassium Channel, TASK-1, May Contribute to an Atrial Substrate for Arrhythmogenesis. *J. Mol. Cell. Cardiol.* **2014**, *67*, 69−76.
(69) Kiper, A. K.; Rinné, S.; Rolfes, C.; Ramírez, D.; Seebohm, G.; Netter, M. F.; González, W.; Decher, N. Kv1.5 Blockers Preferentially

DOI: 10.1021/acs.jmedchem.9b00248
J. Med. Chem. XXXX, XXX, XXX−XXX

Inhibit TASK-1 Channels: TASK-1 as a Target against Atrial Fibrillation and Obstructive Sleep Apnea? *Pfluegers Arch.* **2015**, *467* (5), 1081−1090.
(70) Schmidt, C.; Wiedmann, F.; Voigt, N.; Zhou, X. B.; Heijman, J.; Lang, S.; Albert, V.; Kallenberger, S.; Ruhparwar, A.; Szabó, G.; et al. Upregulation of $K_{2P}3.1$ K^+ Current Causes Action Potential Shortening in Patients with Chronic Atrial Fibrillation. *Circulation* **2015**, *132* (2), 82−92.
(71) Pisani, D. F.; Beranger, G. E.; Corinus, A.; Giroud, M.; Ghandour, R. A.; Altirriba, J.; Chambard, J.-C.; Mazure, N. M.; Bendahhou, S.; Duranton, C.; et al. The K^+ Channel TASK1 Modulates β-Adrenergic Response in Brown Adipose Tissue through the Mineralocorticoid Receptor Pathway. *FASEB J.* **2016**, *30* (2), 909−922.
(72) Bohnen, M. S.; Roman-Campos, D.; Terrenoire, C.; Jnani, J.; Sampson, K. J.; Chung, W. K.; Kass, R. S. The Impact of Heterozygous KCNK3 Mutations Associated With Pulmonary Arterial Hypertension on Channel Function and Pharmacological Recovery. *J. Am. Heart Assoc.* **2017**, *6* (9), e006465.
(73) Friedrich, C.; Rinné, S.; Zumhagen, S.; Kiper, A. K.; Silbernagel, N.; Netter, M. F.; Stallmeyer, B.; Schulze-Bahr, E.; Decher, N. Gain-of-Function Mutation in TASK-4 Channels and Severe Cardiac Conduction Disorder. *EMBO Mol. Med.* **2014**, *6* (7), 937−951.
(74) Wiedmann, F.; Kiper, A. K.; Bedoya, M.; Ratte, A.; Rinné, S.; Kraft, M.; Waibel, M.; Anad, P.; Wenzel, W.; González, W.; et al. Identification of the A293 (AVE1231) Binding Site in the Cardiac Two-Pore-Domain Potassium Channel TASK-1: A Common Low Affinity Antiarrhythmic Drug Binding Site. *Cell. Physiol. Biochem.* **2019**, *52* (5), 1223−1235.
(75) Ramírez, D.; Bedoya, M.; Kiper, A. K.; Rinné, S.; Morales-Navarro, S.; Hernández-Rodríguez, E. W.; Sepúlveda, F. V.; Decher, N.; González, W. Structure/Activity Analysis of TASK-3 Channel Antagonists Based on a 5,6,7,8 Tetrahydropyrido[4,3-d]Pyrimidine. *Int. J. Mol. Sci.* **2019**, *20* (9), 2252.
(76) Aryal, P.; Abd-Wahab, F.; Bucci, G.; Sansom, M. S. P.; Tucker, S. J. Influence of Lipids on the Hydrophobic Barrier within the Pore of the TWIK-1 K2P Channel. *Channels* **2015**, *9* (1), 44−49.
(77) Brennecke, J. T.; de Groot, B. L. Mechanism of Mechanosensitive Gating of the TREK-2 Potassium Channel. *Biophys. J.* **2018**, *114* (6), 1336−1343.
(78) Czirják, G.; Fischer, T.; Spät, A.; Lesage, F.; Enyedi, P. TASK (TWIK-Related Acid-Sensitive K^+ Channel) Is Expressed in Glomerulosa Cells of Rat Adrenal Cortex and Inhibited by Angiotensin II. *Mol. Endocrinol.* **2000**, *14* (6), 863−874.
(79) Meadows, H. J.; Randall, A. D. Functional Characterisation of Human TASK-3, an Acid-Sensitive Two-Pore Domain Potassium Channel. *Neuropharmacology* **2001**, *40* (4), 551−559.
(80) Talley, E. M.; Lei, Q.; Sirois, J. E.; Bayliss, D. A. TASK-1, a Two-Pore Domain K^+ Channel, Is Modulated by Multiple Neurotransmitters in Motoneurons. *Neuron* **2000**, *25* (2), 399−410.
(81) Millar, J. A.; Barratt, L.; Southan, A. P.; Page, K. M.; Fyffe, R. E. W.; Robertson, B.; Mathie, A. A Functional Role for the Two-Pore Domain Potassium Channel TASK-1 in Cerebellar Granule Neurons. *Proc. Natl. Acad. Sci. U. S. A.* **2000**, *97* (7), 3614−3618.
(82) Maingret, F.; Patel, A. J.; Lazdunski, M.; Honoré, E. The Endocannabinoid Anandamide Is a Direct and Selective Blocker of the Background K^+ Channel TASK-1. *EMBO J.* **2001**, *20* (1−2), 47−54.
(83) Czirják, G.; Enyedi, P. TASK-3 Dominates the Background Potassium Conductance in Rat Adrenal Glomerulosa Cells. *Mol. Endocrinol.* **2002**, *16* (3), 621−629.
(84) Patel, A. J.; Honoré, E.; Lesage, F.; Fink, M.; Romey, G.; Lazdunski, M. Inhalational Anesthetics Activate Two-Pore-Domain Background K^+ Channels. *Nat. Neurosci.* **1999**, *2* (5), 422−426.
(85) Luethy, A.; Boghosian, J. D.; Srikantha, R.; Cotten, J. F. Halogenated Ether, Alcohol, and Alkane Anesthetics Activate TASK-3 Tandem Pore Potassium Channels Likely through a Common Mechanism. *Mol. Pharmacol.* **2017**, *91* (6), 620−629.
(86) Tian, F.; Qiu, Y.; Lan, X.; Li, M.; Yang, H.; Gao, Z. A Small-Molecule Compound Selectively Activates K2P Channel TASK-3 by Acting at Two Distant Clusters of Residues. *Mol. Pharmacol.* **2019**, *96* (1), 26−35.
(87) Nayak, T. K.; Harinath, S.; Nama, S.; Somasundaram, K.; Sikdar, S. K. Inhibition of Human Two-Pore Domain K^+ Channel TREK1 by Local Anesthetic Lidocaine: Negative Cooperativity and Half-of-Sites Saturation Kinetics. *Mol. Pharmacol.* **2009**, *76* (4), 903−917.
(88) Kindler, C. H.; Yost, C. S.; Gray, A. T. Local Anesthetic Inhibition of Baseline Potassium Channels with Two Pore Domains in Tandem. *Anesthesiology* **1999**, *90* (4), 1092−1102.
(89) Kindler, C. H.; Paul, M.; Zou, H.; Liu, C.; Winegar, B. D.; Gray, A. T.; Yost, C. S. Amide Local Anesthetics Potently Inhibit the Human Tandem Pore Domain Background K^+ Channel TASK-2 (KCNK5). *J. Pharmacol. Exp. Ther.* **2003**, *306* (1), 84−92.
(90) Kim, D. Physiology and Pharmacology of Two-Pore Domain Potassium Channels. *Curr. Pharm. Des.* **2005**, *11* (21), 2717−2736.
(91) Bang, H.; Kim, Y.; Kim, D. TREK-2, a New Member of the Mechanosensitive Tandem-Pore K^+ Channel Family. *J. Biol. Chem.* **2000**, *275* (23), 17412−17419.
(92) Clarke, C. E.; Veale, E. L.; Wyse, K.; Vandenberg, J. I.; Mathie, A. The M1P1 Loop of TASK3 K2P Channels Apposes the Selectivity Filter and Influences Channel Function. *J. Biol. Chem.* **2008**, *283* (25), 16985−16992.
(93) Putzke, C.; Wemhöner, K.; Sachse, F. B.; Rinné, S.; Schlichthörl, G.; Li, X. T.; Jaé, L.; Eckhardt, I.; Wischmeyer, E.; Wulf, H.; et al. The Acid-Sensitive Potassium Channel TASK-1 in Rat Cardiac Muscle. *Cardiovasc. Res.* **2007**, *75* (1), 59−68.
(94) Miller, M. R.; Zou, B.; Shi, J.; Flaherty, D. P.; Simpson, D. S.; Yao, T.; Maki, B. E.; Day, V. W.; Douglas, J. T.; Wu, M.; et al. Development of a Selective Chemical Inhibitor for the Two-Pore Potassium Channel, KCNK9. *Probe Reports from the NIH Molecular Libraries Program [Internet]*; National Center for Biotechnology Information (U.S.): Bethesda, MD, 2010.
(95) Noriega-Navarro, R.; Lopez-Charcas, O.; Hernández-Enríquez, B.; Reyes-Gutiérrez, P. E.; Martínez, R.; Landa, A.; Morán, J.; Gomora, J. C.; Garcia-Valdes, J. Novel TASK Channels Inhibitors Derived from Dihydropyrrolo[2,1-a]Isoquinoline. *Neuropharmacology* **2014**, *79*, 28−36.
(96) Cotten, J. F.; Keshavaprasad, B.; Laster, M. J.; Eger, E. I.; Yost, C. S. The Ventilatory Stimulant Doxapram Inhibits TASK Tandem Pore (K_{2P}) Potassium Channel Function but Does Not Affect Minimum Alveolar Anesthetic Concentration. *Anesth. Analg.* **2006**, *102* (3), 779−785.
(97) Bruner, J. K.; Zou, B.; Zhang, H.; Zhang, Y.; Schmidt, K.; Li, M. Identification of Novel Small Molecule Modulators of $K_{2P}18.1$ Two-Pore Potassium Channel. *Eur. J. Pharmacol.* **2014**, *740*, 603−610.
(98) Cotten, J. F. TASK-1 (KCNK3) and TASK-3 (KCNK9) Tandem Pore Potassium Channel Antagonists Stimulate Breathing in Isoflurane-Anesthetized Rats. *Anesth. Analg.* **2013**, *116* (4), 810−816.
(99) Zou, B.; Flaherty, D. P.; Simpson, D. S.; Maki, B. E.; Miller, M. R.; Shi, J.; Wu, M.; McManus, O. B.; Golden, J. E.; Aubé, J.; et al. ML365: Development of Bis-Amides as Selective Inhibitors of the KCNK3/TASK1 Two Pore Potassium Channel. In *Probe Reports from the NIH Molecular Libraries Program [Internet]*; National Center for Biotechnology Information (U.S.): Bethesda, MD, 2010.
(100) Wright, P. D.; Veale, E. L.; McCoull, D.; Tickle, D. C.; Large, J. M.; Ococks, E.; Gothard, G.; Kettleborough, C.; Mathie, A.; Jerman, J. Terbinafine Is a Novel and Selective Activator of the Two-Pore Domain Potassium Channel TASK3. *Biochem. Biophys. Res. Commun.* **2017**, *493* (1), 444−450.
(101) Wu, J.; Shih, H. P.; Vigont, V.; Hrdlicka, L.; Diggins, L.; Singh, C.; Mahoney, M.; Chesworth, R.; Shapiro, G.; Zimina, O.; et al. Neuronal Store-Operated Calcium Entry Pathway as a Novel Therapeutic Target for Huntington's Disease Treatment. *Chem. Biol.* **2011**, *18* (6), 777−793.
(102) Sanz, L. M.; Jiménez-Díaz, M. B.; Crespo, B.; De-Cozar, C.; Almela, M. J.; Angulo-Barturen, I.; Castañeda, P.; Ibañez, J.;

DOI: 10.1021/acs.jmedchem.9b00248
J. Med. Chem. XXXX, XXX, XXX−XXX

Fernández, E. P.; Ferrer, S.; et al. Cyclopropyl Carboxamides, a Chemically Novel Class of Antimalarial Agents Identified in a Phenotypic Screen. *Antimicrob. Agents Chemother.* **2011**, *55* (12), 5740−5745.
(103) Saxe, J. P.; Wu, H.; Kelly, T. K.; Phelps, M. E.; Sun, Y. E.; Kornblum, H. I.; Huang, J. A Phenotypic Small-Molecule Screen Identifies an Orphan Ligand-Receptor Pair That Regulates Neural Stem Cell Differentiation. *Chem. Biol.* **2007**, *14* (9), 1019−1030.
(104) Meadows, L. S.; Isom, L. L. Sodium Channels as Macromolecular Complexes: Implications for Inherited Arrhythmia Syndromes. *Cardiovasc. Res.* **2005**, *67* (3), 448−458.
(105) Maffie, J.; Rudy, B. Weighing the Evidence for a Ternary Protein Complex Mediating A-Type K^+ Currents in Neurons. *J. Physiol.* **2008**, *586* (23), 5609−5623.
(106) Wang, Y.; Brittain, J. M.; Jarecki, B. W.; Park, K. D.; Wilson, S. M.; Wang, B.; Hale, R.; Meroueh, S. O.; Cummins, T. R.; Khanna, R. In Silico Docking and Electrophysiological Characterization of Lacosamide Binding Sites on Collapsin Response Mediator Protein-2 Identifies a Pocket Important in Modulating Sodium Channel Slow Inactivation. *J. Biol. Chem.* **2010**, *285* (33), 25296−25307.
(107) Améen, C.; Strehl, R.; Björquist, P.; Lindahl, A.; Hyllner, J.; Sartipy, P. Human Embryonic Stem Cells: Current Technologies and Emerging Industrial Applications. *Crit. Rev. Oncol. Hematol.* **2008**, *65* (1), 54−80.
(108) Sartipy, P.; Björquist, P.; Strehl, R.; Hyllner, J. The Application of Human Embryonic Stem Cell Technologies to Drug Discovery. *Drug Discovery Today* **2007**, *12* (17−18), 688−699.
(109) Ojeda, P. G.; Ramírez, D.; Alzate-Morales, J.; Caballero, J.; Kaas, Q.; González, W. Computational Studies of Snake Venom Toxins. *Toxins* **2018**, *10* (1), 8.
(110) Sabogal-Arango, A.; Barreto, G. E.; Ramírez-Sánchez, D.; González-Mendoza, J.; Barreto, V.; Morales, L.; González, J. Computational Insights of the Interaction among Sea Anemones Neurotoxins and Kv1.3 Channel. *Bioinf. Biol. Insights* **2014**, *8*, 73−81.
(111) Teichert, R. W.; Olivera, B. M. Natural Products and Ion Channel Pharmacology. *Future Med. Chem.* **2010**, *2* (5), 731−744.
(112) Molinski, T. F.; Dalisay, D. S.; Lievens, S. L.; Saludes, J. P. Drug Development from Marine Natural Products. *Nat. Rev. Drug Discovery* **2009**, *8* (1), 69−85.
(113) Buell, G.; Chessell, I. P.; Michel, A. D.; Collo, G.; Salazzo, M.; Herren, S.; Gretener, D.; Grahames, C.; Kaur, R.; Kosco-Vilbois, M. H.; et al. Blockade of Human P2X7 Receptor Function with a Monoclonal Antibody. *Blood* **1998**, *92* (10), 3521−3528.
(114) Mochly-Rosen, D.; Fuchs, S. Monoclonal Anti-Acetylcholine-Receptor Antibodies Directed against the Cholinergic Binding Site. *Biochemistry* **1981**, *20* (20), 5920−5924.
(115) Ramírez, D. Computational Methods Applied to Rational Drug Design. *Open Med. Chem. J.* **2016**, *10* (1), 7−20.
(116) Wermuth, C. G.; Ganellin, C. R.; Lindberg, P.; Mitscher, L. A. Glossary of Terms Used in Medicinal Chemistry (IUPAC Recommendations 1998). *Pure Appl. Chem.* **1998**, *70* (5), 1129−1143.
(117) Yang, S. Y. Pharmacophore Modeling and Applications in Drug Discovery: Challenges and Recent Advances. *Drug Discovery Today* **2010**, *15* (11−12), 444−450.
(118) Dror, O.; Schneidman-Duhovny, D.; Inbar, Y.; Nussinov, R.; Wolfson, H. J. Novel Approach for Efficient Pharmacophore-Based Virtual Screening: Method and Applications. *J. Chem. Inf. Model.* **2009**, *49* (10), 2333−2343.
(119) Huang, Q.; Li, L. L.; Yang, S. Y. PhDD: A New Pharmacophore-Based de Novo Design Method of Drug-like Molecules Combined with Assessment of Synthetic Accessibility. *J. Mol. Graphics Modell.* **2010**, *28* (8), 775−787.
(120) Viswanath, A. N. I.; Jung, S. Y.; Hwang, E. M.; Park, K. D.; Lim, S. M.; Min, S. J.; Cho, Y. S.; Pae, A. N. Identification of the First in Silico-Designed TREK1 Antagonists That Block Channel Currents Dose Dependently. *Chem. Biol. Drug Des.* **2016**, *88* (6), 807−819.
(121) Golder, F. J.; Dax, S.; Baby, S. M.; Gruber, R.; Hoshi, T.; Ideo, C.; Kennedy, A.; Peng, S.; Puskovic, V.; Ritchie, D.; et al. Identification and Characterization of GAL-021 as a Novel Breathing Control Modulator. *Anesthesiology* **2015**, *123* (5), 1093−1104.
(122) Campagna-Slater, V.; Arrowsmith, A. G.; Zhao, Y.; Schapira, M. Pharmacophore Screening of the Protein Data Bank for Specific Binding Site Chemistry. *J. Chem. Inf. Model.* **2010**, *50* (3), 358−367.
(123) Shelke, S. M.; Bhosale, S. H.; Dash, R. C.; Suryawanshi, M. R.; Mahadik, K. R. Exploration of New Scaffolds as Potential MAO-A Inhibitors Using Pharmacophore and 3D-QSAR Based in Silico Screening. *Bioorg. Med. Chem. Lett.* **2011**, *21* (8), 2419−2424.
(124) Dixon, S. L.; Smondyrev, A. M.; Rao, S. N. PHASE: A Novel Approach to Pharmacophore Modeling and 3D Database Searching. *Chem. Biol. Drug Des.* **2006**, *67* (5), 370−372.
(125) Schewe, M.; Sun, H.; Mert, Ü.; Mackenzie, A.; Pike, A. C. W.; Schulz, F.; Constantin, C.; Vowinkel, K. S.; Conrad, L. J.; Kiper, A. K.; et al. A Pharmacological Master Key Mechanism That Unlocks the Selectivity Filter Gate in K^+ Channels. *Science* **2019**, *363* (6429), 875−880.

DOI: 10.1021/acs.jmedchem.9b00248
J. Med. Chem. XXXX, XXX, XXX−XXX